THE JOURNAL OF BIOLOGICAL CHEMISTRY VOL. 288, NO. 12, pp. 8566–8574, March 22, 2013

WNK1 Protein Kinase Regulates Embryonic Cardiovascular Development through the OSR1 Signaling Cascade*

Received for publication, January 8, 2013, and in revised form, January 29, 2013 Published, JBC Papers in Press, February 5, 2013, DOI 10.1074/jbc.M113.451575

Jian Xie[‡], Joonho Yoon[‡], Sung-Sen Yang[§], Shih-Hua Lin[§], and Chou-Long Huang[‡1]

From the [‡]Department of Medicine, University of Texas Southwestern Medical Center at Dallas, Dallas, Texas 75390-8856 and the [§]Department of Medicine, Tri-Service General Hospital, National Defense Medical Center, Taipei 114, Taiwan

Background: WNK1 is critical for embryonic cardiovascular development.
Results: A global deletion of *Osr1* in mice phenocopies the *Wnk1* deletion; expression of the constitutively active mutant OSR1 rescues developmental defects in *Wnk1*-null embryos.
Conclusion: WNK1 activation of OSR1 is essential for mouse embryo development.
Significance: The WNK1-OSR1 signaling cascade is a novel pathway that regulates embryonic angiogenesis and cardiac formation.

WNK1 is a widely expressed serine/threonine protein kinase that regulates multiple cellular and organ functions via diverse mechanisms. We previously reported that endothelial-specific deletion of *Wnk1* in mice results in embryonic lethality, with angiogenesis and cardiac defects beginning at embryonic day ~10.5. Here, we further investigated the signaling mechanism by which WNK1 regulates embryonic cardiovascular development. We found that mice with a global deletion of *Osr1*, which encodes oxidative stress-responsive kinase-1, a protein kinase activated by WNK1, died *in utero* beginning at embryonic day ~11. The defects in *Osr1*-null yolk sacs and embryos were virtually identical to those observed in *Wnk1*-knock-out mice: no mature large vessels in yolk sacs, defective angiogenesis in the brain and intersomitic vessels, and smaller chambers and reduced myocardial trabeculation in mutant hearts. Endothelial-specific deletion of *Osr1* generated by crossing $Osr1^{flox/flox}$ mice with *Tie2-Cre* mice phenocopied defects caused by global *Osr1* deletion. To investigate whether OSR1 acts downstream of WNK1 in embryonic angiogenesis, we generated a mouse line that carries a catalytically and constitutively active human *OSR1* transgene in the *ROSA26* locus under the control of a cassette of floxed transcription stop codons. We found that endothelial-specific expression of the constitutively active mutant OSR1, generated by *Tie2-Cre*-mediated excision of floxed stop codons in the mutated *ROSA26* locus, rescued angiogenesis and cardiac defects in global *Wnk1*-null embryos. These results indicate that WNK1 activation of the OSR1 signaling cascade is an essential pathway that regulates angiogenesis and cardiac formation during mouse embryo development.

WNK1 (with no lysine (K) 1) is a member of the family of serine/threonine protein kinases characterized by the unique placement of the catalytic lysine (1). There are four mammalian members of the WNK kinase family, WNK1–4, each encoded by a separate gene (1–3). The WNK1 protein is >2100 amino acids long; WNK2–4 are between 1200 and 1800 amino acids in length. The four WNK kinases share a conserved kinase domain, an autoinhibitory domain, one to two coiled-coil domains, and multiple proline-rich motifs for potential protein-protein interactions. Outside these recognizable motifs, the amino acid sequences of WNK kinases are not well conserved. Despite the atypical kinase domain structure, WNKs are *bona fide* protein kinases and catalyze phosphorylation of endogenous substrates (4).

The functions of WNK kinases were first revealed by the discovery that mutations in *WNK1* and *WNK4* in humans cause the autosomal dominant disease pseudohypoaldosteronism type 2, which is characterized by hypertension and hyperkalemia (2). Subsequent studies have shown that WNK1 and WNK4 play important roles in the regulation of ion transport proteins involved in Na^+ and K^+ homeostasis (4). Regulation involves kinase activity-dependent as well as activity-independent mechanisms. With respect to kinase-dependent mechanisms, WNK1 and WNK4 activate SPAK (Ste20-related proline/alanine-rich kinase) and OSR1 (oxidative stress-responsive kinase-1) by conferring phosphorylation on a critical threonine residue in the catalytic loop and probably also on a serine in the regulatory domain (5–8). In turn, activated OSR1 and SPAK can phosphorylate and activate cation-chloride cotransporters NCC and NKCC1/2 to regulate renal Na^+ reabsorption and vascular smooth muscle contractility (5–8). Through kinase-independent events, WNK1 binds and somehow activates SGK kinase, causing it to increase surface expression of the epithelial Na^+ channel (9); and WNK1 and WNK4 interact with the endocytic scaffold protein intersectin to enhance endocytosis of the renal K^+ channel ROMK (10). Dysregulation of Na^+ and K^+ transport in the kidney contributes to the hypertension and hyperkalemia of pseudohypoaldosteronism type 2.

WNK1 also regulates intracellular signaling. WNK1 activates ERK5, and knockdown of WNK1 decreases activation of ERK5 by epidermal growth factor receptors (11). More recently, it has

* This work was supported, in whole or in part, by National Institutes of Health Grants DK59530, DK85726, and DK79328. This work was also supported Taiwan National Science Council Grant NSC-100-2314-B016-018-MY3.
[1] To whom correspondence should be addressed: Dept. of Medicine, UT Southwestern Medical Center, 5323 Harry Hines Blvd., Dallas, TX 75390-8856. Tel.: 214-648-8627; Fax: 214-648-2071; E-mail: chou-long.huang@utsouthwestern.edu.

been shown that WNK1 plays an important role in G protein-coupled receptor and phospholipase C signaling (12). WNK1 stimulates phospholipase Cβ signaling by promoting the synthesis of phosphatidylinositol 4,5-bisphosphate via stimulation of phosphatidylinositol 4-kinase IIIα, and this regulation is amplified when WNK1 is phosphorylated by Akt kinase. This new signaling mechanism allows crosstalk between G protein-coupled receptors and Akt-activating growth factors and provides a way to independently control phospholipase C signaling and membrane phosphatidylinositol 4,5-bisphosphate availability.

Another important function of WNK1 is in embryonic development. Mice homozygous for *Wnk1* inactivation die during embryonic development (13). We have recently shown that *Wnk1*-ablated mice die *in utero* from cardiac developmental and angiogenesis defects (14). The defects in *Wnk1*-null embryos are distinct from abnormalities observed in embryos with disruption of known angiogenesis pathways, *e.g.* VEGF and Notch signaling pathways, and are not associated with alterations of expression of genes in these pathways. In this study, we demonstrate that deletion of *Osr1* in endothelial cells virtually phenocopied defects of *Wnk1*-deleted embryos and that endothelial-specific expression of constitutively active OSR1 rescued cardiovascular defects in *Wnk1*-deleted embryos. These findings indicate that WNK1 activation of OSR1 is a novel pathway essential for embryonic cardiovascular development in mice.

EXPERIMENTAL PROCEDURES

Mouse Strains and Genotyping—$Wnk1^{+/-}$, $Wnk1^{flox/+}$, *Tie2-Cre* transgenic, *Sox2-Cre* transgenic, $Osr1^{+/-}$, and $Osr1^{flox/+}$ mice have been described (14, 15). All animal maintenance and experiments were conducted in accordance with the Guide for the Use and Care of Laboratory Animals and approved by the Institutional Animal Care and Use Committee of University of Texas Southwestern Medical Center at Dallas. For timed breeding, the appearance of a vaginal plug was checked twice a day at 9 a.m. and 6 p.m., and 1 a.m. or 1 p.m. of the day in which a plug was found was designated as embryonic day 0, respectively. The embryonic stage was further confirmed by the number of somites at the time of embryo dissection. For genotyping, mouse tail tips, ear punches, toe clips, or portions of yolk sacs of embryos were digested overnight in Viagen DirectPCR® reagents with 0.2 mg/ml proteinase K at 55 °C; heat-inactivated at 85 °C for 45 min; and analyzed by PCRs as described (14). All genotyping PCRs were performed with 35 cycles at 95 °C for 20 s, 60 °C for 20 s, and 72 °C for 30 s. The primers for genotyping of *Wnk1*-knock-out and *Cre* mice were as described (14, 15). The primer sequences used for *Osr1*-knock-out genotyping (see Fig. 1*B*) were AAACCTGCTGGGCTTCTATG (forward) and TGGGGTTAGTGGGGATAAGA (reverse); those used for $Osr1^{flox}$ conditional knock-out genotyping (see Fig. 4*B*) were TGTTTCCAGCTATCCAGAGTGA (forward) and TGGTGAAATGGCAAATGTGT (reverse); and those used for genotyping the targeted *ROSA26-*$hOSR1^{ca}$ allele (see Fig. 5*B*) were CCCCCTGAACCTGAAACATA (F1), GAGTTCTCTGCTGCCTCCTG (F2), and AAGCTGCTTGGACTACAGCAGTTGC (R1).

ROSA26-$hOSR1^{ca}$ *Targeting and Rescue*—A mutant human *OSR1* cDNA encoding the constitutively active form of OSR1 kinase ($hOSR1^{ca}$) was generated by mutating Thr-185 and Ser-325 to a phosphomimicking glutamate (T185E and S325E) by site-directed mutagenesis. The mutant $hOSR1^{ca}$ cDNA was amplified using two primers (sense, CTAGCTAGCATGTCCGAGGACTCGAGCGC, with the NheI site underlined; and antisense, AGGCCCGGGTTAGCTGATGCTGAGCTGGGC, with the ApaI site underlined). The amplified 1.58-kb fragment was subcloned into the pBigT plasmid in multiple cloning sites downstream of loxP-PGKneo-tpA-loxP. The resulting pBigT-$hOSR1^{ca}$ construct was digested with PacI-AscI and inserted between the short and long arms of the *ROSA26* genomic sequence in the pROSA plasmid (16) to create the *ROSA26-*$hOSR1^{ca}$ targeting vector. After linearization with SwaI, the targeting vector was introduced into 129S6 embryonic stem cells by electroporation. G418-resistant embryonic stem cells were digested with Viagen reagent and proteinase as described above and then screened for the targeted *ROSA26-*$hOSR1^{ca}$ allele by PCR. PCR primers consisted of a forward primer located upstream of the *ROSA26* short arm (AGGTAGGGGATCGGGACTCT) and a reverse primer in the 5′-loxP site of the targeting vector (GCAGGTCGAGGGACCTAATA). Another reverse primer located in the *ROSA26* short arm (TAAGCCTGCCCAGAAGACTC) was included in the reaction for internal PCR control. PCR was performed with HotStarTaq (Qiagen) and 35 cycles at 95 °C for 30 s, 60 °C for 30 s, and 72 °C for 2 min. The PCR product for the wild-type *ROSA26* allele was ~1.2 kb; the product for the targeted *ROSA26-*$hOSR1^{ca}$ allele was ~1.4 kb (data not shown). The positive clones were expanded and injected into C57BL/6 blastocysts to generate chimeric founders. Culture and electroporation of embryonic stem cells and injection of embryonic stem cells into blastocysts were carried out in the Transgenic Core Facility of the University of Texas Southwestern Medical Center. More than 30 male chimeras with 80–100% agouti coat color were backcrossed with C57BL/6 females, and germ-line transmission was determined by the presence of agouti offspring and confirmed by genotyping PCR.

Histology and Immunohistochemistry—For routine histological analysis, embryos were fixed overnight with 4% paraformaldehyde at 4 °C. Thereafter, they were stored in 50% ethanol solution and embedded in paraffin wax for sectioning and hematoxylin and eosin staining. Whole-mount immunostaining by anti-PECAM1 (platelet endothelial cell adhesion molecule-1) antibodies (at 1:300 dilution) was performed as described (14) with modifications. Signal was detected using a biotinylated secondary antibody (at 1:500 dilution) and a VECTASTAIN Elite ABC kit (Vector Laboratories).

Quantitative Real-time PCR—Total RNAs were extracted from tissues (embryo, yolk sac, kidney, etc.) using TRIzol (Invitrogen). 1 μg of DNase-treated RNAs was reverse-transcribed using a TaqMan reverse transcription kit (Applied Biosystems). The resulting cDNA samples were analyzed by regular PCR or quantitative real-time PCR using SYBR PCR reagents (Bio-Rad) and the real-time PCR system from Applied Biosystems.

TABLE 1
Distribution of E9.5–13.5 embryos and pups from heterozygous *Osr1* crossing
ab, live abnormal (defective) embryos; d, dead embryos.

Age	Total	+/+	+/−	−/−
E9.5	24	6 (25%)	11 (46%)	7 (29%)
E10	17	4 (24%)	8 (47%)	5[ab] (29%)
E10.5	20	3 (15%)	9 (45%)	8[ab] (40%)
E11.5	23	9 (39%)	13 (57%)	1[d] (4%)
E12.5	15	4 (27%)	8 (53%)	3[d] (20%)
E13.5	19	4 (21%)	10 (53%)	5[d] (26%)
Pups	67	21 (31%)	46 (69%)	0 (0%)

RESULTS

$Osr1^{-/-}$ Embryos Die between Embryonic Days 10.5 and 11.5 with Cardiovascular Defects—Deletion of *Osr1* in mice causes embryonic lethality (15). To examine the cause of death of *Osr1*-deleted embryos, we examined phenotypes of timed embryos by crossing heterozygous *Osr1*-knock-out mice and collected embryos at various embryonic stages. Viable homozygous *Osr1*-deleted embryos ($Osr1^{-/-}$) were obtained with the expected Mendelian ratios at embryonic days (E)[2] 9.5–10.5 (Table 1; see Fig. 1*B* for genotyping). At E9.5, the homozygous embryos were normal and phenotypically indistinguishable from their wild-type and heterozygous littermates. However, $Osr1^{-/-}$ embryos started to show growth retardation beginning at E10 (five of five abnormal at E10 and eight of eight abnormal at E10.5) (Table 1). All $Osr1^{-/-}$ embryos at the embryonic stage between E11.5 and E13.5 were dead, and no $Osr1^{-/-}$ embryos were recovered beyond E13.5.

Compared with wild-type embryos, $Osr1^{-/-}$ embryos at E10.5 exhibited growth retardation of varying severity, with pericardial edema (Fig. 1*A*, *black arrows*) and hemorrhage in various locations, including around the heart (*yellow arrows*), common cardinal veins, and the head. Despite a smaller overall size, the body axis and somite number of living $Osr1^{-/-}$ mutant embryos at E10.5 were similar to those of wild-type embryos (Fig. 1*A*). $Osr1^{+/-}$ embryos were phenotypically indistinguishable from wild-type embryos (data not shown). Wild-type yolk sacs at E10.5 showed a network of large and small vessels filled with circulating blood (Fig. 1*A*, *white arrow*). In contrast, yolk sacs of E10.5 mutants were noticeably thinner and paler and lacked larger branching vitelline vessels and blood circulation (Fig. 1*A*).

The death of embryos at midgestation, lack of detectable blood circulation and large vessels in the mutant yolk sac, hemorrhage, and pericardial edema are all indicative of cardiovascular developmental defects. To analyze cardiovascular defects, we sectioned the embryos and examined the histology of hearts and blood vessels. In Fig. 2 (*A* and *B*), the transverse sections through the hearts of E10.5 wild-type and $Osr1^{-/-}$ embryos revealed hypoplasia of atrial (*a*) and ventricular (common ventricle (*cv*) and bulbus cordis (*bc*)) chambers in mutant embryos compared with wild-type embryos. The myocardial trabeculations in the developing ventricular chambers were extensive in wild-type embryos but were significantly reduced in mutants. Pericardial edema was evident from the dilatation of the pericardial sac (Fig. 2*B*, *arrowhead*). Thus, *Osr1*-ablated embryos

[2] The abbreviation used is: E, embryonic day.

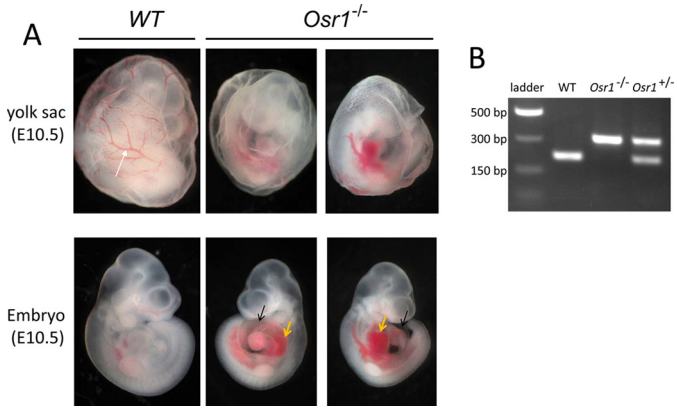

FIGURE 1. **Gross morphology of wild-type and *Osr1*-knock-out mouse embryos and yolk sacs at E10.5.** *A*, compared with wild-type embryos, $Osr1^{-/-}$ embryos were growth-retarded, and yolk sac lacked visible big vessels (*white arrow*). Hemorrhage in the head, heart, and common cardinal vein area (*yellow arrows*) and pericardial edema were present in $Osr1^{-/-}$ embryos. *B*, genotyping PCR analysis of wild-type, $Osr1^{-/-}$, and $Osr1^{+/-}$ embryos.

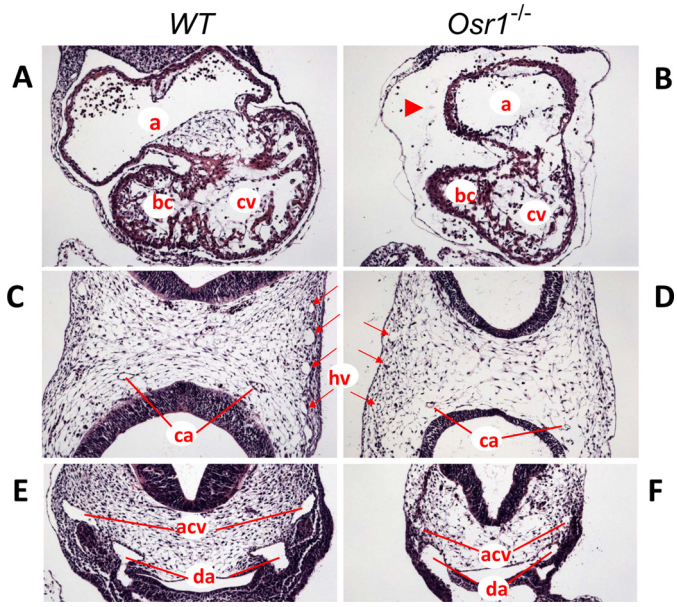

FIGURE 2. **Cross-sections of E10.5 wild-type and $Osr1^{-/-}$ embryos stained with hematoxylin and eosin.** Wild-type (*A*, *C*, and *E*) and $Osr1^{-/-}$ (*B*, *D*, and *F*) embryos were cross-sectioned at different levels. The developing hearts of mutant embryos (*B*) were smaller in size and had much less trabeculation and enlarged pericardial-peritoneal cavities compared with wild-type embryos (*A*). *a*, common atrium; *cv*, common ventricle; *bc*, bulbus cordis. In the head regions, the internal carotid artery (*ca*) and primary head veins (*hv*) were either smaller or missing in mutant embryos (*D*) compared with wild-type embryos (*C*). In the trunks, anterior cardinal veins (*acv*) and dorsal aortas (*da*) were smaller in mutant embryos (*F*) compared with wild-type embryos (*E*).

exhibited defective heart development, including reduced heart chamber size and reduced myocardial trabeculation. In addition, in Fig. 2 (*C* and *D*), the cross-sections of wild-type and mutant embryos revealed collapsed head veins (*hv*) and carotid arteries (*ca*) and much smaller dorsal aortas (*da*) and anterior cardinal veins (*acv*) in the mutants.

PECAM1 Immunostaining Reveals Angiogenesis Defects in $Osr1^{-/-}$ Embryos—We further examined embryonic vascular development by whole-mount immunostaining of embryos using an antibody against a pan-endothelial cell marker, PECAM1. Formation of the vasculature framework was evident by PECAM1 immunostaining in both wild-type and *Osr1*-null

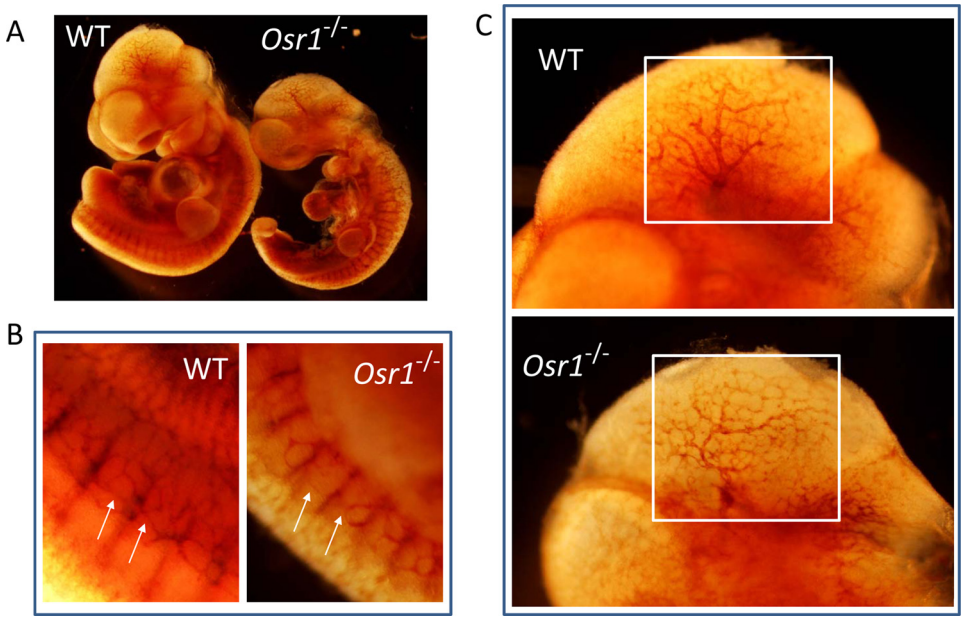

FIGURE 3. **Whole-mount PECAM staining of E10.5 embryos reveals angiogenesis defects in *Osr1*$^{-/-}$ mutants.** *A*, a major framework of blood vessels formed in mutant embryos but was less organized, and the density of vessels was lower compared with wild-type embryos. *B*, enlarged view showing irregular patterning and reduced branching of intersomitic vessels (*arrows*) in a mutant embryo compared with a wild-type embryo. *C*, enlarged view showing disorganized vessels in the head region of a mutant embryo compared with a wild-type embryo.

mutant embryos at E10.5 (Fig. 3*A*). However, the density of blood vessels was lower, and their organization was defective in mutant embryos compared with wild-type embryos (Fig. 3, *B* and *C*). In wild-type embryos, intersomitic vessels displayed a distinct pattern and complexity with multiple branches (Fig. 3*B*, *arrows*). In contrast, the intersomitic vessels of mutant embryos were disorganized and reduced in number, with irregular patterning and poor branching. Similarly, the density of vessels and sprouting and branching of vessels in the head region were markedly reduced in mutant embryos compared with wild-type embryos (Fig. 3*C*, *box*).

Endothelial-specific Conditional Knock-out of Osr1 Phenocopies Developmental Defects Caused by Global Osr1 Ablation—Non-endothelial cell types surrounding developing vasculature also play critical roles in angiogenesis (17). To define the cell lineages in which OSR1 function is essential for cardiovascular development, we generated conditional knock-out of *Osr1* in endothelial cells by crossing *Osr1*-floxed mice with a *Tie2-Cre* transgenic mouse line that expresses Cre recombinase specifically in endothelial cell lineages (18). We found that some *Osr1*$^{flox/flox}$;*Tie2-Cre* embryos started to show growth defects and abnormality similar to the global *Osr1*-null embryos from E10.5 (Table 2; see also Fig. 4). The percentage of abnormal *Osr1*$^{flox/flox}$;*Tie2-Cre* embryos increased at E11.5–12.5, with the presence of dead mutant embryos. At E13.5, *Osr1*$^{flox/flox}$;*Tie2-Cre* embryos were either dead or severely defective (Table 2). No live *Osr1*$^{flox/flox}$;*Tie2-Cre* embryos were recovered beyond E13.5. Also, as in global *Osr1*$^{-/-}$ mutants, the yolk sac vasculature failed to remodel in E10.5 *Osr1*$^{flox/flox}$;*Tie2-Cre* mutants (Fig. 4*A*; see Fig. 4*B* for genotyping). *Osr1*$^{flox/flox}$;*Tie2-Cre* embryos were growth-retarded and displayed hemorrhage in multiple regions and pericardial edema compared with *Osr1*$^{flox/flox}$ embryos. *Osr1*$^{flox/flox}$ embryos were phenotypically indistinguishable from wild-type embryos.

TABLE 2
Distribution of *Osr1*$^{flox/flox}$;*Tie2-Cre* embryos and pups from *Osr1*$^{flox/flox}$ × *Osr1*$^{flox/+}$;*Tie2-Cre* intercrossing
ab, live abnormal (defective) embryos; d, dead embryos.

Age	Total	*Osr1*$^{flox/flox}$ (25% expected)	*Osr1*$^{flox/flox}$;*Tie2-Cre* (25% expected)
E9.5	36	10 (28%)	7 (19%)
E10.5	42	12 (29%)	10 (24%, 4^{ab})
E11.5	23	7 (30%)	5 (22%, 3^{ab} + 1^{d})
E12.5	51	14 (27%)	9 (18%, 3^{ab} + 4^{d})
E13.5	37	12 (32%)	6 (16%, 2^{ab} + 4^{d})
E14.5–16.5	67	25 (37%)	4^{d} (6%)
Pups	107	34 (32%)	0 (0%)

Conditional Expression of a Constitutively Active hOSR1 Transgene—To study the function of OSR1 kinase in different tissues and cell lineages independently of its upstream activator(s), we generated a mouse line that allows for tissue-specific expression of activated OSR1 under the control of Cre recombinase. Phosphorylation by WNK kinases at Thr-185 and Ser-325 activates OSR1 kinase (5–8). Mutations of either or both residues to glutamate render OSR1 constitutively active independently of WNK kinases (5–8, 19). We mutated both threonine and serine residues to glutamate and placed the mutant human *OSR1* transgene (*hOSR1*^{ca}) in the transcriptionally active mouse *ROSA26* locus behind a cassette of floxed transcription terminator codons (Fig. 5*A*). Mice carrying the *ROSA26-hOSR1*^{ca} allele will express constitutively active OSR1 in tissues of interest when crossed with transgenic mice expressing tissue-specific Cre recombinase. As shown, when *ROSA26-hOSR1*^{ca} mice were crossed with a ubiquitous *Sox2-Cre* mouse line, only the cleaved form of *ROSA26-hOSR1*^{ca} was detected in the genotyping PCR of mouse tail DNA, indicating that the targeted allele was activated globally (Fig. 5*B*, *second lane*). In contrast, when *ROSA26-hOSR1*^{ca} mice were crossed with *Tie2-Cre* mice, both cleaved and uncleaved forms of *ROSA26-hOSR1*^{ca} were detected in the genotyping PCR analy-

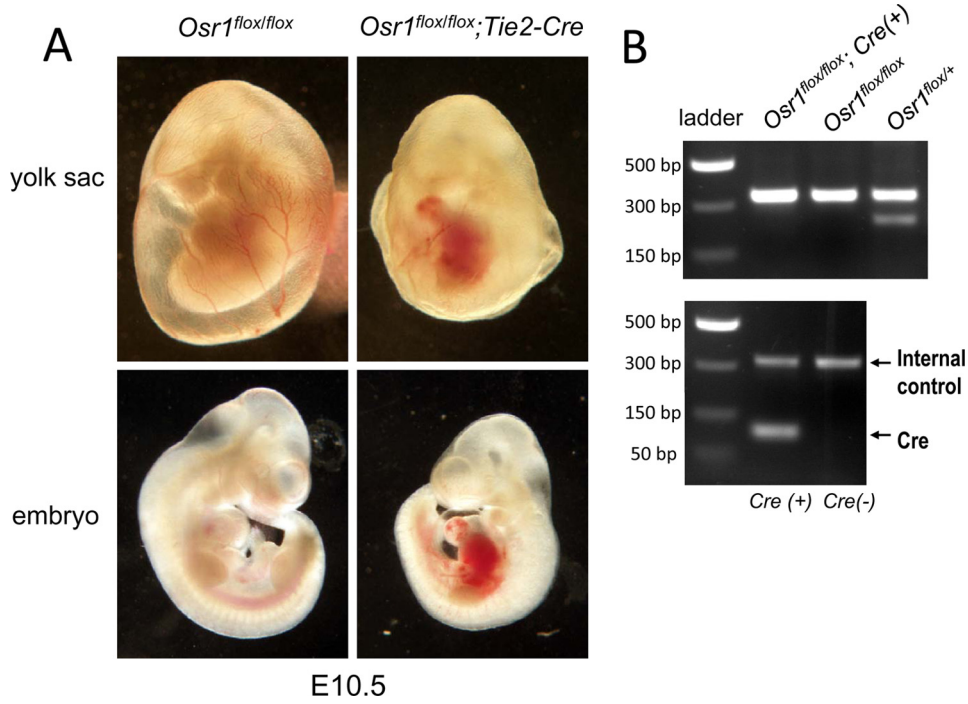

FIGURE 4. **Yolk sac and embryo proper of endothelial-specific knock-out of *Osr1* at E10.5.** *A*, *upper panels*, the yolk sac of an $Osr1^{flox/flox}$;*Tie2-Cre* embryo had defective angiogenesis compared with an $Osr1^{flox/flox}$ embryo. *Lower panels*, an $Osr1^{flox/flox}$;*Tie2-Cre* embryo was growth-retarded and smaller than an $Osr1^{flox/flox}$ embryo. *B*, genotyping PCR analysis of $Osr1^{flox/flox}$;Cre^{+}, $Osr1^{flox/flox}$, and $Osr1^{flox/+}$ embryos. *Upper panel*, genotyping for the $Osr1^{flox}$ allele. *Lower panel*, genotyping for the *Cre* allele.

sis, consistent with the notion that the transgene was cleaved and activated in the endothelial cells and the uncleaved form was present in other tissues (Fig. 5*B*, *third lane*). The expression of exogenous $hOSR1^{ca}$ cDNA in the kidneys of *ROSA26-*$hOSR1^{ca}$;*Sox2-Cre* mice but not of wild-type mice was confirmed by RT-PCR using primers specific for human *OSR1*, which detected the cDNA of the transgene (Fig. 5*C*, *lanes 1* and *2*). For comparison, primers that recognize sequence conserved between $hOSR1^{ca}$ cDNA and endogenous mouse *Osr1* cDNA detected signals in both *ROSA26-*$hOSR1^{ca}$;*Sox2-Cre* and wild-type mice (Fig. 5*C*, *lanes 3* and *4*).

We next tested the ability of Cre recombinase-mediated excised $hOSR1^{ca}$ cDNA to substitute for the function of OSR1 in *Osr1*-knock-out mice by intercrossing of *ROSA26-*$hOSR1^{ca}$;*Sox2-Cre*;$Osr1^{+/-}$ mice with $Osr1^{+/-}$ mice. The intercrossing generated *ROSA26-*$hOSR1^{ca}$;*Sox2-Cre*;$Osr1^{-/-}$ offspring with the expected Mendelian ratios (data not shown), indicating that transgenic expression of $hOSR1^{ca}$ rescued the embryonic lethality caused by *Osr1* deletion. The rescued mice were fertile and grossly normal, with no apparent morphological difference compared with wild-type littermates (Fig. 5*D*). Quantitative real-time PCR of adult kidney mRNAs (using primers targeting the exons that are deleted in *Osr1*-knock-out mice but that are conserved between mouse *Osr1* and human *OSR1* sequences) confirmed the expression of $hOSR1^{ca}$ in rescued mice, and the level was ~2-fold relative to the level of endogenous *Osr1* mRNA in wild-type mice (Fig. 5*E*). As expected, the *Osr1* mRNA was reduced in the *Osr1* heterozygotes.

Rescue of Developmental Defects in $Wnk1^{-/-}$ *Embryos by* $hOSR1^{ca}$ *Transgene Expression*—Having validated the expression of $hOSR1^{ca}$ by Cre recombinase, we next tested whether expression of activated OSR1 can rescue the developmental defects in $Wnk1^{-/-}$ mice. *Wnk1* and *ROSA26* alleles are both located on mouse chromosome 6, only ~6.9 megabases apart. To increase the frequency of obtaining the desired genotypes from breeding, we first intercrossed $Wnk1^{+/-}$ and *ROSA26-*$hOSR1^{ca}$ mice to create $Wnk1^{+/-}$;*ROSA26-*$hOSR1^{ca}$ double heterozygous mice in which the *Wnk1* mutant locus and the *ROSA26-*$hOSR1^{ca}$ transgene locus were initially on different chromatids (Fig. 6*A*). These mice were then repeatedly bred with wild-type mice to generate [$Wnk1^{+/-}$;*ROSA26-*$hOSR1^{ca}$] mice, in which the two loci became "linked" on the same chromatid through chromosomal crossover. Further crossing of these mice with $Wnk1^{+/-}$;Cre^{+} animals generated a population of $Wnk1^{+/-}$;*ROSA26-*$hOSR1^{ca}$ mice that were 12.5% frequency-positive and 12.5% frequency-negative for *Cre* (Fig. 6*A*). Fig. 6*B* shows the results from genotyping PCR analysis of the *Wnk1* allele.

Table 3 shows the results of intercrossing of [$Wnk1^{+/-}$; *ROSA26-*$hOSR1^{ca}$] mice with $Wnk1^{+/-}$;*Tie2-Cre* mice analyzed at different embryonic stages. Note that the distribution of $Wnk1^{-/-}$;*ROSA26-*$hOSR1^{ca}$ embryos with either $Tie2\text{-}Cre^{+}$ or $Tie2\text{-}Cre^{-}$ negative at E10.5–11.5 follows the expected Mendelian ratios (*i.e.* ~12.5% each). Overall, this intercrossing produced a total of 22 $Wnk1^{-/-}$;*ROSA26-*$hOSR1^{ca}$ (Cre^{+} or Cre^{-}) embryos from a total of 169 embryos collected between E10.5 and E18.5. Among these, five embryos were $Tie2\text{-}Cre^{-}$ and either dead or defective by E13.5; 17 embryos were $Tie2\text{-}Cre^{+}$. 7 of 17 $Wnk1^{-/-}$;*ROSA26-*$hOSR1^{ca}$;*Tie2-Cre* embryos were recovered at E12.5–13.5, and among these, two were normal phenocopies of wild-type embryos at E13.5 (Table 3 and Fig. 6*C*). In separate experiments in which we crossed unlinked

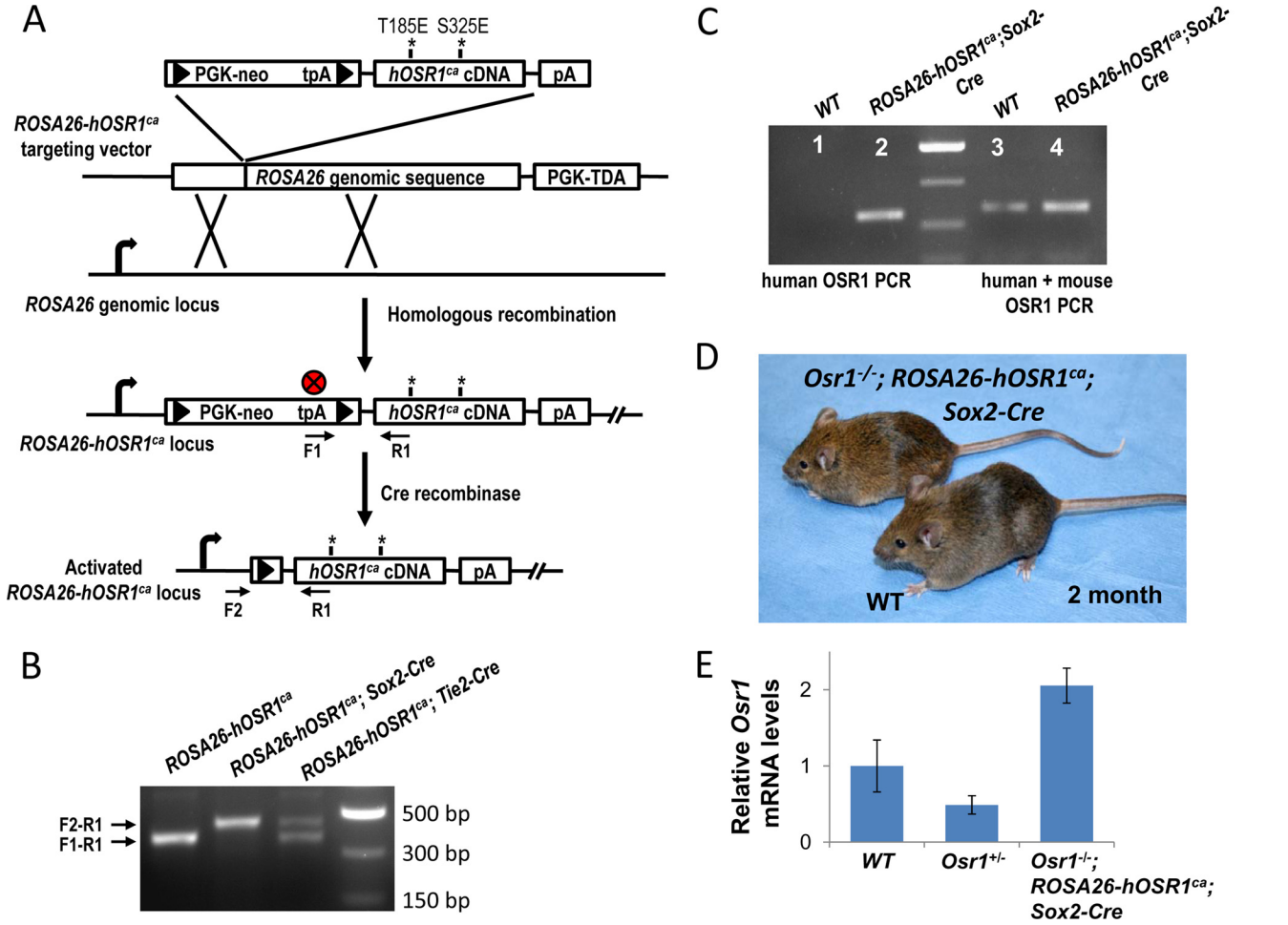

FIGURE 5. **Conditional expression of catalytically and constitutively active OSR1 in mice.** *A*, targeting scheme. A mutant human *OSR1* cDNA encoding the constitutively active form of OSR1 kinase (*hOSR1^{ca}*) was made by site-directed mutagenesis of Thr-185 and Ser-325 to a phosphomimicking glutamate (T185E and S325E). The cDNA was inserted downstream of a loxP-flanking (*triangle*) triple-poly(A) site (*tpA*). This fragment was targeted into a constitutively transcribing *ROSA26* locus to generate *ROSA26-hOSR1^{ca}* mice. When crossed with transgenic *Cre*-expressing mice, Cre-mediated excision would delete the triple-poly(A) site so that *hOSR1^{ca}* was expressed tissue-specifically in the *Cre^{+}* progeny. *B*, genotyping PCR analysis of different *ROSA26-hOSR1^{ca}* mice. Primer F1 targets the inserted poly(A) sites, primer F2 is upstream of the inserted cassette, and primer R1 targets the *hOSR1^{ca}* cDNA. PCR using these two sets of primers detected the unexcised *ROSA26-hOSR1^{ca}* locus in *Cre^{-}* mice (*first lane*), the Cre-excised locus in mice expressing ubiquitous *Sox2-Cre* (*second lane*), and both excised and unexcised forms in the endothelial-specific *Tie2-Cre*-expressing mice (*third lane*). *C*, PCR analysis reveals the expression of *hOSR1^{ca}* in kidney. Human OSR1-specific primers (forward, aatgatttcattgtgccttca; and reverse, tggaacctggtactctccgc) detected *hOSR1^{ca}* cDNA in *ROSA26-hOSR1^{ca};Sox2-Cre* mice (*lane 2*) but not in wild-type mice (*lane 1*). Primers targeting the *OSR1* sequence conserved between mouse and human (forward, aatgatttcattgtgccttca; and reverse, tcactccactcccagcctcc) detected endogenous mouse *Osr1* cDNA in wild-type mice (*lane 3*) and both *Osr1* and *hOSR1^{ca}* in *ROSA26-hOSR1^{ca};Sox2-Cre* mice (*lane 4*). *D*, *Osr1$^{-/-}$; ROSA26-hOSR1^{ca};Sox2-Cre* mice were viable and appeared identical to wild-type littermates at 2 month of age. *E*, quantitative real-time PCR analysis of kidney RNAs with primers targeting the deleted exon 10 in *Osr1*-knock-out mice. As expected, the *Osr1* mRNA level in *Osr1$^{+/-}$* mice was about half that in wild-type mice. Expression of *hOSR1^{ca}* in *Osr1$^{-/-}$;ROSA26-hOSR1^{ca};Sox2-Cre* mice was ~2-fold of that *Osr1* mRNA in wild-type mice. The forward and reverse PCR primers used were aatgatttcattgtgccttca and tcactccactcccagcctcc, respectively.

Wnk1$^{+/-}$;ROSA26-hOSR1^{ca} mice with *Wnk1$^{+/-}$;Tie2-Cre* mice, we found that *Wnk1$^{+/+}$;ROSA26-hOSR1^{ca};Tie2-Cre* embryos were phenotypically indistinguishable from wild-type embryos (data not shown). We have found that, without genetic rescue, all *Wnk1$^{-/-}$* embryos are dead by E12.5 (14). These results indicate that transgenic expression of *hOSR1^{ca}* in endothelial cells could rescue cardiovascular defects of *Wnk1* knock-out. Because the expression *Osr1* is not altered in *Wnk1*-knock-out embryos (Fig. 6*D*), the effect of rescue is likely due to constitutive activation of OSR1 kinase activity. The developing hearts and other organs (including the lung, liver, kidney, and gastrointestinal tract) of the E13.5 rescued embryos were largely similar to those of wild-type embryos (data not shown). However, most of the *Wnk1$^{-/-}$;ROSA26-hOSR1^{ca};Tie2-Cre* embryos between E10.5 and E18.5 were dead or defective, and no *Wnk1*-null pups were found (Table 3).

To determine whether the incomplete rescue of developmental defects of *Wnk1*-null mice by *Tie2-Cre*-mediated activation of *hOSR1^{ca}* may be due to a requirement of WNK1-OSR1 signaling in tissues outside endothelial cells, we crossed [*Wnk1$^{+/-}$;ROSA26-hOSR1^{ca}*] mice with *Wnk1$^{+/-}$;Sox2-Cre* mice to see whether the lethality of *Wnk1* knock-out can be rescued by globally expressed active *hOSR1^{ca}*. Of 215 new born pups (days 0–7), we found 19 *Wnk1$^{-/-}$* pups, and all of them were positive for *Sox2-Cre* (Table 4). The frequency of *Wnk1$^{-/-}$* pups rescued by *Sox2-Cre*-mediated activated OSR1 was ~9%, not markedly different from that expected. However, a large percentage of live born pups died within the first few

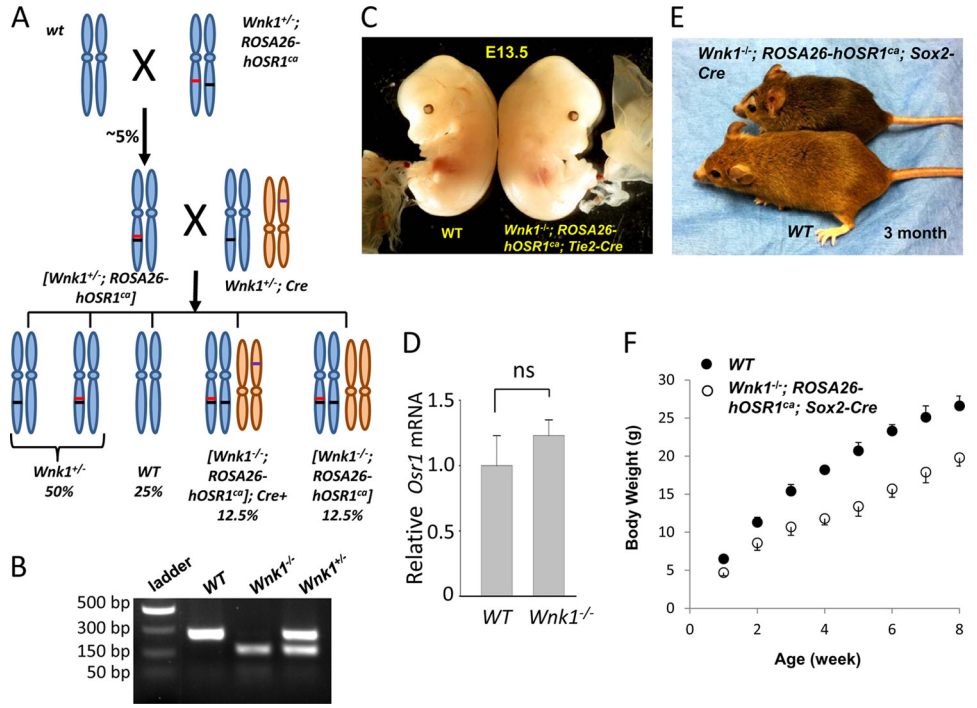

FIGURE 6. **Expression of *hOSR1^{ca}* rescues *Wnk1*-knock-out mice.** *A*, breeding scheme for *Wnk1*-knock-out rescue. The initial breeding between *Wnk1*$^{+/-}$ and *ROSA26-hOSR1^{ca}* mice (not illustrated here) produced mice carrying both alleles in two separate chromatids. The *Wnk1* and *ROSA26* loci in mice are both located on chromosome 6, only ~6.9 megabases apart. To increase the frequency of progeny with both alleles, we bred mice carrying both *Wnk1*$^{+/-}$ and *ROSA26-hOSR1^{ca}* alleles in separate chromatids with wild-type mice to generate mice in which the two loci were linked on the same chromosome, *i.e.* [*Wnk1*$^{+/-}$;*ROSA26-hOSR1^{ca}*] mice. Crossing these mice with *Wnk1*$^{+/-}$;*Cre*$^{+}$ mice produced *Wnk1*$^{-/-}$ progeny carrying *ROSA26-hOSR1^{ca}* with 25% frequency. Among them, half were *Cre*$^{+}$, and half were *Cre*$^{-}$ (12.5% each). *B*, genotyping PCR analysis for wild-type, *Wnk1*$^{-/-}$, and *Wnk1*$^{+/-}$. *C*, a live and normal *Wnk1*$^{-/-}$;*ROSA26-hOSR1^{ca}*; *Tie2-Cre* embryo at E13.5 appeared to be identical to its wild-type littermate. *D*, *Osr1* mRNA levels in E9.0 *Wnk1*-null embryos (relative to wild-type embryos) analyzed by quantitative real-time PCR (n = four each). *ns*, not significant. *E*, a *Wnk1*$^{-/-}$; *ROSA26-hOSR1^{ca}*;*Sox2-Cre* mouse at 3 months of age was smaller than its wild-type littermate. *F*, growth curve of *Wnk1*$^{-/-}$;*ROSA26-hOSR1^{ca}*;*Sox2-Cre* mice compared with wild-type controls.

TABLE 3

Distribution of *Wnk1*$^{-/-}$;*ROSA26-hOSR1^{ca}*;*Tie2-Cre* embryos and pups from *Wnk1*$^{+/-}$;*Tie2-Cre* × [*Wnk1*$^{+/-}$;*ROSA26-hOSR1^{ca}*] intercrossing

Note that *Wnk1* and *ROSA26-hOSR1^{ca}* alleles are linked on the same chromosome. ab, live abnormal (defective) embryos; d, dead embryos.

Age	Total	*Tie2-Cre*$^{-}$ (12.5% expected)	*Tie2-Cre*$^{+}$ (12.5% expected)
E10.5–11.5	26	3 (11.5%, $1^{ab} + 2^{d}$)	4 (14.4%, 2^{ab})
E12.5–13.5	65	2 (3.1%, 2^{d})	7 (10.8%, $3^{ab} + 2^{d}$)
E14.5–16.5	47	0 (0%)	4 (8.5%, $1^{ab} + 3^{d}$)
E17.5–18.5	31	0 (0%)	2 (6.5%, 2^{d})
Pups	84	0 (0%)	0 (0%)

TABLE 4

Distribution of *Wnk1*$^{-/-}$;*ROSA26-hOSR1^{ca}*;*Sox2-Cre* pups from [*Wnk1*$^{+/-}$;*Sox2-Cre* × *Wnk1*$^{+/-}$;*ROSA26-hOSR1^{ca}*] intercrossing

Note that *Wnk1* and *ROSA26-hOSR1^{ca}* alleles are linked on the same chromosome. *d*, dead embryos.

Age	Total	*Sox2-Cre*$^{-}$ (12.5% expected)	*Sox2-Cre*$^{+}$ (12.5% expected)
Pups			
Days 0–1	126	0 (0%)	12 (9.5%, 7^{d})
Days 2–7	89	0 (0%)	7 (7.9%, 4^{d})
Adults (>30 days)	184	0 (0%)	6 (3.3%, runted)

days after birth, and only ~3% of adult mice were *Wnk1*$^{-/-}$ and *Sox2-Cre*$^{+}$. Those that survived to adulthood were growth-retarded compared with wild-type littermates of the same gender (Fig. 6, *E* and *F*). Thus, activation of OSR1 by WNK1 in other tissues besides the endothelium may be required for embryonic development. Alternatively, the recombination frequency of *Sox2-Cre* may be higher compared with *Tie2-Cre* in endothelial cells. The perinatal death and growth retardation suggest that a function(s) of WNK1 independent of OSR1 is necessary for postnatal growth and organ function(s) of adult mice. Of note, the gross morphology and body weight of *Wnk1*$^{+/+}$;*ROSA26-hOSR1^{ca}*;*Sox2-Cre* pups and adult mice up to 8 weeks old (from intercrossing between unlinked *Wnk1*$^{+/-}$;*ROSA26-hOSR1^{ca}* and *Wnk1*$^{+/-}$;*Sox2-Cre* mice) were indistinguishable from those of wild-type littermates (data not shown). Whether transgenic expression of constitutively active OSR1 alters organ function later in life awaits future studies.

DISCUSSION

Embryonic vascular development occurs via two separate processes (20, 21). Vasculogenesis results in the formation of the primordial heart tube and major axial vessels as well as the primary vessels in the embryo proper and extraembryonic structures such as the yolk sac. The second process, angiogenesis, is responsible for the formation of blood vessels in organs such as the brain and kidney through further growth, sprouting, branching, and remodeling of the primary vessels. Angiogenesis defects can also lead to cardiac developmental defects (22, 23). We have previously reported that WNK1 function in endothelial cells is critical for embryonic angiogenesis and cardiac development (14). The signaling pathways for the regulation were unknown. Here, we have demonstrated that endothelial-specific deletion of OSR1, a downstream kinase activated by WNK1, phenocopies *Wnk1*-deleted embryos. Expression of a constitutively active *OSR1* transgene in endothelial cells res-

cued cardiovascular defects of *Wnk1*-deleted embryos. These results provide compelling evidence to support the hypothesis that WNK1 regulates embryonic cardiovascular development in mice by activation of OSR1 signaling in endothelial cells.

Two previous studies also reported that OSR1 is important for embryogenesis. Rafiqi *et al.* (24) generated knock-in mice carrying a T185A mutation in the T-loop of OSR1. Delpire and Gagnon (8) described another loss-of-function OSR1 mouse model created by gene-trap insertion in exon 15. In both models, the mice died before term. Detailed analysis of timing of death was not performed in either study, but some embryos were recovered at E17.5. This apparent timing of death is later than what we observed in *Osr1*-deleted mice (approximately E10.5–11.5). Studies have show that T185A mutant OSR1 does not phosphorylate and activate NKCC1 in response to WNK1 in *Xenopus* oocytes and in *in vitro* assay (5, 6), yet WNK1 kinase is capable of phosphorylating T185A mutant OSR1 at Ser-325 in the S-motif (5). Gene-trap insertion in exon 15 resulted in partial loss of amino acids in the conserved C terminus of OSR1 known to be important for interacting with its substrates and other proteins (8). Our knock-out mice were generated by targeted deletion of exons 9 and 10 of *Osr1*, which results in truncation of the kinase domain and loss of kinase activity (15). The expression of endogenous *Osr1* is not altered in *Wnk1*-deleted mice. Our finding that catalytically and constitutively active OSR1 rescues phenotypes of *Wnk1* deletion argues against the idea that OSR1 regulates angiogenesis independently of its kinase activity. Thus, the apparent delayed lethality in the knock-in and gene-trap mice may be due to residual kinase activity of OSR1 *in vivo*. Alternatively, OSR1 may also function as a scaffold and thereby contribute to the regulation of embryogenesis.

Many molecules have been identified to play critical roles in regulating vascular development. These include growth factors and their receptors (VEGF, Flt1, Flk1, etc.), factors that activate the Notch signaling pathway, angiopoietins, ephrins, neuropilins, transcription factor COUP-TFII, integrins, extracellular matrices, and proteases (20–23). We found that expression of many of these known factors is not altered in $Wnk1^{-/-}$ embryos (14). Consistent with the notion of a non-transcriptional mechanism for WNK1 regulation of angiogenesis, our current findings suggest that WNK1-regulated embryonic cardiovascular development involves activation of the downstream kinase OSR1. Members of the SLC family of ion transporters such as the sodium-potassium-chloride cotransporters NKCC1 and NKCC2 and the sodium-chloride cotransporter NCC are substrates for OSR1 (4–8). These sodium transporters are unlikely to be the downstream mediators of the WNK1-OSR1 signaling pathway in embryonic cardiovascular development because deletion of these genes does not cause embryonic developmental defects (25–27). Conceivably, OSR1 may phosphorylate and regulate function of the abovementioned angiogenesis factors such as VEGF, angiopoietins, ephrins, and COUP-TFII.

Alternatively, OSR1 may regulate angiogenesis through PAKs (p21-activated kinases). PAKs are effector proteins for the Rho family of small GTPases and important regulators of cellular processes involving actin cytoskeletal dynamics (28). Studies have found that PAKs modulate multiple endothelial cell processes critical for angiogenesis, including proliferation, sprouting, migration, and lumen formation and maturation (29–31). Deletion of *Pak4* and functional inactivation of *Pak2* in mice both cause embryonic lethality at approximately E10.5, and these mutant embryos exhibit embryonic and extraembryonic vascular formation defects resembling *Wnk1* and *Osr1* knock-out (32, 33), as we have observed. OSR1 phosphorylates PAK1 and alters its activation by Cdc42 (34). Future studies will need to investigate whether OSR1 activates PAK2 and/or PAK4 to regulate embryonic vascular development.

Acknowledgments—We thank Dr. M. Cobb for the human OSR1 cDNA; Dr. T. Carroll for the pBigT and pROSA plasmids; and Drs. Cobb, O. Cleaver, and A. Rodan for discussions and comments.

REFERENCES

1. Xu, B., English, J. M., Wilsbacher, J. L., Stippec, S., Goldsmith, E. J., and Cobb, M. H. (2000) WNK1, a novel mammalian serine/threonine protein kinase lacking the catalytic lysine in subdomain II. *J. Biol. Chem.* **275,** 16795–16801
2. Wilson, F. H., Disse-Nicodème, S., Choate, K. A., Ishikawa, K., Nelson-Williams, C., Desitter, I., Gunel, M., Milford, D. V., Lipkin, G. W., Achard, J. M., Feely, M. P., Dussol, B., Berland, Y., Unwin, R. J., Mayan, H., Simon, D. B., Farfel, Z., Jeunemaitre, X., and Lifton, R. P. (2001) Human hypertension caused by mutations in WNK kinases. *Science* **293,** 1107–1112
3. Veríssimo, F., and Jordan, P. (2001) WNK kinases, a novel protein kinase subfamily in multi-cellular organisms. *Oncogene* **20,** 5562–5569
4. McCormick, J. A., and Ellison, D. H. (2011) The WNKs: atypical protein kinases with pleiotropic actions. *Physiol. Rev.* **91,** 177–219
5. Vitari, A. C., Deak, M., Morrice, N. A., and Alessi, D. R. (2005) The WNK1 and WNK4 protein kinases that are mutated in Gordon's hypertension syndrome phosphorylate and activate SPAK and OSR1 protein kinases. *Biochem. J.* **391,** 17–24
6. Moriguchi, T., Urushiyama, S., Hisamoto, N., Iemura, S., Uchida, S., Natsume, T., Matsumoto, K., and Shibuya, H. (2005) WNK1 regulates phosphorylation of cation-chloride-coupled cotransporters via the STE20-related kinases, SPAK and OSR1. *J. Biol. Chem.* **280,** 42685–42693
7. Anselmo, A. N., Earnest, S., Chen, W., Juang, Y. C., Kim, S. C., Zhao, Y., and Cobb, M. H. (2006) WNK1 and OSR1 regulate the Na^+,K^+,$2Cl^-$ cotransporter in HeLa cells. *Proc. Natl. Acad. Sci. U.S.A.* **103,** 10883–10888
8. Delpire, E., and Gagnon, K. B. (2008) SPAK and OSR1: STE20 kinases involved in the regulation of ion homoeostasis and volume control in mammalian cells. *Biochem. J.* **409,** 321–331
9. Xu, B. E., Stippec, S., Chu, P. Y., Lazrak, A., Li, X. J., Lee, B. H., English, J. M., Ortega, B., Huang, C. L., and Cobb, M. H. (2005) WNK1 activates SGK1 to regulate the epithelial sodium channel. *Proc. Natl. Acad. Sci. U.S.A.* **102,** 10315–10320
10. He, G., Wang, H. R., Huang, S. K., and Huang, C. L. (2007) Intersectin links WNK kinases to endocytosis of ROMK. *J. Clin. Invest.* **117,** 1078–1087
11. Xu, B. E., Stippec, S., Lenertz, L., Lee, B. H., Zhang, W., Lee, Y. K., and Cobb, M. H. (2004) WNK1 activates ERK5 by an MEKK2/3-dependent mechanism. *J. Biol. Chem.* **279,** 7826–7831
12. An, S. W., Cha, S. K., Yoon, J., Chang, S., Ross, E. M., and Huang, C. L. (2011) WNK1 promotes PIP_2 synthesis to coordinate growth factor and GPCR-G_q signaling. *Curr. Biol.* **21,** 1979–1987
13. Zambrowicz, B. P., Abuin, A., Ramirez-Solis, R., Richter, L. J., Piggott, J., BeltrandelRio, H., Buxton, E. C., Edwards, J., Finch, R. A., Friddle, C. J., Gupta, A., Hansen, G., Hu, Y., Huang, W., Jaing, C., Key, B. W. Jr., Kipp, P., Kohlhauff, B., Ma, Z. Q., Markesich, D., Payne, R., Potter, D. G., Qian, N., Shaw, J., Schrick, J., Shi, Z. Z., Sparks, M. J., Van Sligtenhorst, I., Vogel, P., Walke, W., Xu, N., Zhu, Q., Person, C., and Sands, A. T. (2003) Wnk1 kinase deficiency lowers blood pressure in mice: A gene-trap screen to

identify potential targets for therapeutic intervention. *Proc. Natl. Acad. Sci. U.S.A.* **100,** 14109–14114
14. Xie, J., Wu, T., Xu, K., Huang, I. K., Cleaver, O., and Huang, C.-L. (2009) Endothelial expression of WNK1 is essential for angiogenesis and cardiovascular development in mice. *Am. J. Pathol.* **175,** 1315–1327
15. Lin, S. H., Yu, I. S., Jiang, S. T., Lin, S. W., Chu, P., Chen, A., Sytwu, H. K., Sohara, E., Uchida, S., Sasaki, S., and Yang, S. S. (2011) Impaired phosphorylation of Na^+-K^+-$2Cl^-$ cotransporter by oxidative stress-responsive kinase-1 deficiency manifests hypotension and Bartter-like syndrome. *Proc. Natl. Acad. Sci. U.S.A.* **108,** 17538–17543
16. Srinivas, S., Watanabe, T., Lin, C. S., William, C. M., Tanabe, Y., Jessell, T. M., and Costantini, F. (2001) Cre reporter strains produced by targeted insertion of *EYFP* and *ECFP* into the *ROSA26* locus. *BMC Dev. Biol.* **1,** 4
17. Coultas, L., Chawengsaksophak, K., and Rossant, J. (2005) Endothelial cells and VEGF in vascular development. *Nature* **438,** 937–945
18. Kisanuki, Y. Y., Hammer, R. E., Miyazaki, J., Williams, S. C., Richardson, J. A., and Yanagisawa, M. (2001) Tie2-Cre transgenic mice: a new model for endothelial cell-lineage analysis *in vivo*. *Dev. Biol.* **230,** 230–242
19. Gagnon, K. B., and Delpire, E. (2010) On the substrate recognition and negative regulation of SPAK, a kinase modulating Na^+-K^+-$2Cl^-$ cotransport activity. *Am. J. Physiol. Cell Physiol.* **299,** C614–C620
20. Risau, W., and Flamme, I. (1995) Vasculogenesis. *Annu. Rev. Cell Dev. Biol.* **11,** 73–91
21. Folkman, J., and D'Amore, P. A. (1996) Blood vessel formation: what is its molecular basis? *Cell* **87,** 1153–1155
22. Wang, H. U., Chen, Z. F., and Anderson, D. J. (1998) Molecular distinction and angiogenic interaction between embryonic arteries and veins revealed by ephrin-B2 and its receptor Eph-B4. *Cell* **93,** 741–753
23. You, L. R., Lin, F. J., Lee, C. T., DeMayo, F. J., Tsai, M. J., and Tsai, S. Y. (2005) Suppression of Notch signaling by the COUP-TFII transcription factor regulates vein identity. *Nature* **435,** 98–104
24. Rafiqi, F. H., Zuber, A. M., Glover, M., Richardson, C., Fleming, S., Jovanović, S., Jovanović, A., O'Shaughnessy, K. M., and Alessi, D. R. (2010) Role of the WNK-activated SPAK kinase in regulating blood pressure. *EMBO Mol. Med.* **2,** 63–75
25. Delpire, E., Lu, J., England, R., Dull, C., and Thorne, T. (1999) Deafness and imbalance associated with inactivation of the secretory Na-K-2Cl co-transporter. *Nat. Genet.* **22,** 192–195
26. Takahashi, N., Chernavvsky, D. R., Gomez, R. A., Igarashi, P., Gitelman, H. J., and Smithies, O. (2000) Uncompensated polyuria in a mouse model of Bartter's syndrome. *Proc. Natl. Acad. Sci. U.S.A.* **97,** 5434–5439
27. Schultheis, P. J., Lorenz, J. N., Meneton, P., Nieman, M. L., Riddle, T. M., Flagella, M., Duffy, J. J., Doetschman, T., Miller, M. L., and Shull, G. E. (1998) Phenotype resembling Gitelman's syndrome in mice lacking the apical Na^+-Cl^- cotransporter of the distal convoluted tubule. *J. Biol. Chem.* **273,** 29150–29155
28. Wells, C. M., and Jones, G. E. (2010) The emerging importance of group II PAKs. *Biochem. J.* **425,** 465–473
29. Kiosses, W. B., Daniels, R. H., Otey, C., Bokoch, G. M., and Schwartz, M. A. (1999) A role for p21-activated kinase in endothelial cell migration. *J. Cell Biol.* **147,** 831–844
30. Koh, W., Mahan, R. D., and Davis, G. E. (2008) Cdc42- and Rac1-mediated endothelial lumen formation requires Pak2, Pak4 and Par3, and PKC-dependent signaling. *J. Cell Sci.* **121,** 989–1001
31. Galan Moya, E. M., Le Guelte, A., and Gavard, J. (2009) PAKing up to the endothelium. *Cell. Signal.* **21,** 1727–1737
32. Marlin, J. W., Chang, Y. W., Ober, M., Handy, A., Xu, W., and Jakobi, R. (2011) Functional PAK-2 knockout and replacement with a caspase cleavage-deficient mutant in mice reveals differential requirements of full-length PAK-2 and caspase-activated PAK-2p34. *Mamm. Genome* **22,** 306–317
33. Tian, Y., Lei, L., Cammarano, M., Nekrasova, T., and Minden, A. (2009) Essential role for the Pak4 protein kinase in extraembryonic tissue development and vessel formation. *Mech. Dev.* **126,** 710–720
34. Chen, W., Yazicioglu, M., and Cobb, M. H. (2004) Characterization of OSR1, a member of the mammalian Ste20p/germinal center kinase subfamily. *J. Biol. Chem.* **279,** 11129–11136